CD2 expression acts as a quantitative checkpoint for immunological synapse structure and T-cell activation.

Philippos Demetriou[1], Enas Abu-Shah[1,2], Sarah McCuaig[1], Viveka Mayya[1,3], Salvatore Valvo[1], Kseniya Korobchevskaya[1], Matthias Friedrich[1], Elizabeth Mann[1], Lennard YW Lee[4], Thomas Starkey[4], Mikhail A. Kutuzov[2], Jehan Afrose[1,3,§], Anastasios Siokis[5], Oxford IBD Cohort Investigators[7], Michael Meyer-Hermann[5,6], David Depoil[1,3, #,*], Michael L. Dustin[1,3,*].

SUPPLEMENTARY INFORMATION

Supplementary Figure 1. CD8 exhaustion signature, CD2 gene expression and levels in CD4$^+$ and CD8$^+$ CRC TILs

The putative negative correlation of T cell exhaustion genesets and CD2 expression described in Figure 1 was then validated using the METALLIC colorectal cancer clinical cohort **a)** The correlation between exhausted CD8$^+$ T-cell gene signature and CD2 expression is shown for (top) "exhausted vs effector CD8$^+$ T cell gene signature" and (bottom) "exhausted vs naive CD8$^+$ T cell gene signature". **b)** The gating strategy for looking at CD127, PD-1 profile of CD3+ TIL subsets. **c)** The mean number of CD2 molecules/cell, for CD4$^+$ TIL subsets from Figure 1(b-c), is shown for each patient. Patients were sorted from highest to lowest CD2 expression of the CD127$^-$PD-1$^+$ CD8$^+$ T-cell compartment. **d)** Comparison of CD2 levels (mean±S.D.) in CD127$^-$PD-1$^+$ CD8$^+$ T-cells of Group A ($4.8 \times 10^4 \pm 7.6 \times 10^3$), 14 patients (from Figure 1, showing the CD2^{low} phenotype) and Group B ($9.0 \times 10^4 \pm 1.5 \times 10^4$), 5 patients CRC with CD2 levels detected in peripheral blood CD8$^+$ T-cell of healthy individuals (naïve, $4.8 \times 10^4 \pm 8.9 \times 10^3$; memory, $7.6 \times 10^4 \pm 8.9 \times 10^3$). ****, $p < 0.0001$; ***, $p < 0.006$ with unpaired two-tailed Mann Whitney test. Error bars represent SEM. **e)** CD2 against PD-1 levels of CD127$^-$PD-1$^+$ CD4$^+$ TILs from (c) are shown for each donor. Dotted line crossing x-axis (with grey rectangle) represents the average PD-1 levels (±SD) expressed in memory PD-1$^+$ CD3$^+$CD4$^+$ T-cells found in peripheral blood of healthy controls. Dashed or dotted line crossing y-axis (with grey rectangle) represents the average CD2 levels (±SD) expressed in naive and memory CD3$^+$CD4$^+$ T-cells, respectively, found in peripheral blood of healthy individuals.

Supplementary Figure 2. A unique ring pattern, "corolla", formed by CD2-CD58 interactions in the IS.

a) Further examples of the CD2 and LFA-1 signal in fixed T:B conjugates as in Figure 1. Shown in 3D rendering (IMARIS software), are T:B cell conjugates (top panels) and 1 µm thick slice of the corresponding T:B cell interface shown in the bottom panels. Images were captured on an Airy-Scan Confocal Microscope (ZEISS). Representative images are shown from two independent experiments. Scale bar, 5 µm. **b)** Representative histograms showing the CD58 expression levels of the human CF996 EBV-transformed B cells (solid empty), human peripheral blood monocytes (light grey), *in vitro* differentiated immature monocyte-derived dendritic cells (dark grey) and *in vitro* maturate monocyte-derived dendritic cells (black). Dotted histogram represents isotype control stained cells. Scale bar, 5 µm.

Supplementary Figure 3. pMHC-induced CD2 corolla captures ligated CD28.

1G4^{+} TCR CD8^{+} T-cells incubated on ICAM-1 ($200/µm^2$), NY-ESO-9V-peptide-loaded HLA-A2 ($30/µm^2$), CD80 ($200/µm^2$) with CD58 ($200/µm^2$) reconstituted SLB and real-time imaged with TIRFM, 10-15 min after contact and/or fixed at 15 min of incubation. Fluorescently labelled streptavidin was used to track the biotinylated NY-ESO-9V-peptide-loaded MHC. A representative image from two independent experiments is shown. Scale bar, 5 µm.

Supplementary Figure 4. CD2 expression determines corolla formation.

a) The gating strategy, in PBMCs, to quantify the levels of surface CD2 in T-cell subsets from healthy individuals is shown. After gating on single and live cells, CD4^{+}CD3^{+} (left) or CD8^{+}CD3^{+} (right) cells were selected and divided into naïve

(CD62L$^+$CD45RA$^+$), central memory (CD62L$^+$CD45RA$^-$), effector memory (CD62L$^-$CD45RA$^-$) and effector memory that re-expressed CD45RA (CD62L$^-$CD45RA$^+$). **b)** The gating strategy for determining transfected human CD2-levels in expanded AND T-cells. **c)** The histograms show an example of AND T-cells transfected with different levels of human CD2 (hCD2FL; full length protein) and compared to CD2 levels found in human peripheral blood T-cells from healthy individuals. Control cells were stained untransfected AND T cells (empty solid line histogram). **d)** Transfected AND T-cells from (c) after a 15 min incubation on ICAM-1 (200/µm^2), MCC-I-E^k (30/µm^2) and CD58 (200/µm^2) reconstituted SLBs, fixed and imaged with TIRFM. The ICAM-1, CD2 and CD58 signals in the IS of a random selection of AND T-cells are shown for one representative of two such experiments. **e)** Same as in (d) but using AND T-cells transfected with hCD2TM (hCD2 lacking its cytoplasmic tail)

Supplementary Figure 5. CD127$^-$PD-1$^+$ CD8$^+$ TILs from CRC patients are enriched in CD28$^-$ TILs while CD127$^-$PD-1$^+$ CD4$^+$ TILs are mainly CD28$^+$.

a) (Left) Representative CD28 and PD-1 expression plots (and gating) in CD127$^-$PD-1$^+$ CD4$^+$ from one CRC patient. (Right) The proportion of CD28 positive (CD28$^+$) and CD28 negative (CD28$^-$) T-cells present within the viable CD127$^-$PD-1$^+$ CD4$^+$ TILs is shown for each CRC patient. **b)** (Left) Representative CD28 and PD-1 expression plots (and gating) in CD127$^-$PD-1$^+$ CD8$^+$ from one CRC patient. (Right) The proportion of CD28 positive (CD28$^+$) and CD28 negative (CD28$^-$) T cells present within the viable CD127$^-$PD-1$^+$ CD8$^+$ TILs is shown for each CRC patient.

Supplementary Movie 1 and 2 (connects to Figure 2)

Tracking of IS formation by a human T-cell incubated on ICAM1 ($200/\mu m^2$), anti-CD3 Fab ($30/\mu m^2$), CD58 ($200/\mu m^2$) reconstituted SLBs. Cells were imaged at 4s intervals with TIRFM. Scale bar

Supplementary Movie 3 (connects to Figure 3)

Tracking of IS formation by a human T-cell incubated on ICAM1 ($200/\mu m^2$), anti-CD3 Fab ($30/\mu m^2$), CD58 ($200/\mu m^2$), CD80 ($100/\mu m^2$) reconstituted SLBs. Cells were imaged at 4s intervals with TIRFM.

Supplementary Table 1a. Clinical characteristics of CRC patients assessed in this study.

Patient ID	Type	Age	Gender	Specific Stage of disease	Tumour side (left or right side?	Is it colon or rectal?	Prognosis/recurrence?
1	CRC	84	M	T4 N1 M0	Right	Ascending colon	pT3 pN0 Ly0 V0 R0. No recurrent or metastatic disease is identified.
2	CRC	70	F	T3 N0 M0	Left	Sigmoid colon	pT3 pN2 Ly0 V0 R0. No evidence of residual or recurrent disease.
3	CRC	75	F	T2N0	Left	Rectosigmoid colon	ypT3 ypN1 Ly0 V1 R0. No evidence of local or distant tumour or nodal recurrence.
4	CRC	65	M	T3 N0 M0	ND	Rectum below perit.reflexion	pT3 pN2 Ly1 V1 R1. Further interval disease progression in multiple lung metastases.
5	CRC	66	M	T3 N2 M0	Right	Caecal cancer	pT3 pN0 Ly0 V0 R0. No evidence of disease recurrence.
6	CRC	71	M	Tx	Right	Transverse colon	pT3 pN0 Ly0 V0 R0. No evidence of disease recurrence
7	CRC	39	M	T2 N0 M0	Left	Rectosigmoid colon	pT3 pN0 Ly0 V0 R0. No metastatic disease.
8	CRC	75	F	T2 N0 M0	ND	Rectum below perit.reflexion	pT2 pN0 Ly1 V0.
9	CRC	84	M	T4 N1 M0	Left	Sigmoid colon	pT4b pN1a Ly1 V1 R0.
10	CRC	68	M	T2 N0 M0	ND	Rectum below perit.reflexion	pT3 pN0 Ly0 V1 R0. New small bowel dilatation and mild small bowel thickening.
11	CRC	55	F	T3 N2 M0	Left	Descending colon	ND
12	CRC	76	F	T4	Right	Transverse colon	pT4b,N0,L0,V0,R0
13	CRC	82	M	T2 N0 M0	Right	Caecum	ND
14	CRC	83	F	T2 N0 M0	Right	Ascending colon	ND

ND, no data available

6

Supplementary Table1a. ctd.

Patient ID	Type	Age	Gender	Specific Stage of disease	Tumour side (left or right side?	Is it colon or rectal?	Prognosis/recurrence?
15	CRC	83	M	T2 N0 M0	Left	Sigmoid colon	ND
16	CRC	76	F	T2 N0 M0	Right	Caecum	ND
17	CRC	81	M	T3 N1 M0	Right	Ascending colon	ND
18	CRC	74	F	T3 N1 Mx	Right	Hepatic flexure tumour	ND
19	CRC	81	F	T2/3a N1 V0 M0.	ND	Rectum below perit.reflexion	ND

ND, no data available

7

Supplementary Table 1b. Clinical characteristics of CRC patients assessed in this study.

Patient ID	Genetic information
1	Mutation detected in the KRAS gene (c.38G>A, p.(Gly13Asp), COSM532). Immunohistochemistry for Mismatch repair proteins show no loss of nuclear staining (MLH1, MSH2, MSH4 and PMS1)
2	Mutation detected in the KRAS gene (c.35G>T, p.(Gly12Val), COSM520). Mutation detected in the TP53 gene (c.267_267delC, p.(Ser90fs), COSM12683330).
3	Mutation not detected in the KRAS, NRAS and BRAF genes. Mutations detected in the TP53 gene (c.841G>A, p.(Asp281Asn), COSM43596) and (c.817C>T, p. (Arg273Cys), COSM10659)
4	Mutation not detected in the KRAS and NRAS genes.
5	Mutation not detected in the KRAS, NRAS and BRAF genes. Mutation detected in the PIK3CA gene (c.3140A>G, p.(His1047Arg), COSM775).
6	Mutation detected in the KRAS gene (c.436G>A, p.(Ala146Thr), COSM194404). Mutations detected in the TP53 gene (c.328C>T, p.(Arg110Cys), COSM43682; c.916C>T, p.(Arg306Ter), COSM10663; and c.413C>T, p.(Ala138Val), COSM43818). Mutations detected in the PIK3CA gene (c.263G>A, p.(Arg88Gln), COSM746 and c.3140A>G, p. (His1047Arg), COSM775).
7	Mutation not detected in the KRAS, NRAS and BRAF genes. Mutation detected in the TP53 gene (c.524G>A, p.(Arg175His), COSM10648).
8	Mutation detected in the KRAS gene (c.35G>T, p.(Gly12Val), COSM520). Mutation not detected in the NRAS and BRAF genes. Mutations detected in the PIK3CA gene (c.1637A>G, p.(Gln546Arg), COSM12459). Mutation detected in the TP53 gene (c.742C>T, p.(Arg248Trp), COSM10656).
9	MMR immunohistochemistry shows intact expression.
10	Clinically significant variant not detected in the KRAS, NRAS or BRAF genes. Variant detected in the TP53 gene (c.832C>A, p.(Pro278Thr), COSM43697).
11	ND
12	Mutation not detected in the KRAS and NRAS genes. Mutation detected in the BRAF gene (c.1799T>A, p.(Val600Glu), COSM476).
13	Mutation detected in the KRAS gene (c.35G>A, p.(Gly12Asp), COSM521).

ND, no data available

Supplementary Table 1b. ctd.

Patient ID	Genetic information
14	Mutation detected in the BRAF gene (c.1799T>A, p.(Val600Glu), COSM476). Presence of BRAF p.(Val600Glu) in the context of loss of MLH1 (IHC) is suggestive, although not conclusive, of a sporadic tumour (Molecular testing strategies for Lynch Syndrome in people with colorectal cancer. Mutation detected in the PIK3CA gene (c.263G>A, p.Arg88Gln), COSM746)
15	Mutation detected in the KRAS gene (c.35G>A, p.(Gly12Asp), COSM521). Mutation detected in the PIK3CA gene (c.1035T>A, p.(Asn345Lys), COSM754).
16	The tumour cells show positive immunostaining for MLH1, MSH2 and PMS2, but are immunonegative for MSH6, suggesting loss of expression.
17	MMR Immunohistochemistry: MLH1: Absent MSH2: Intact MSH6: Absent PMS2: Absent
18	The tumour cells are immunopositive for MSH2 and MSH6, but are negative for MLH1 and PMS2, suggesting loss of expression.
19	Mismatch repair immunostains show no loss of MLH1, PMS2, MSH2 and MSH6 NUCLEAR STAINING.

Supplementary Table 2. CD2 mean expression in natural T-cell subsets in peripheral blood from 12 healthy individuals.

T cell subset	Molecules/cell	(+/-)SD
Naïve CD4+	3.15E+04	4.44E+03
CM CD4+	5.22E+04	7.39E+03
EM CD4+	7.05E+04	1.23E+04
CD45RA+ EM CD4+	4.02E+04	1.34E+04
Naïve CD8+	4.79E+04	8.90E+03
CM CD8+	7.46E+04	7.36E+03
EM CD8+	7.79E+04	1.10E+04
CD45RA+ EM	5.62E+04	1.15E+04
pooled CD45RA- (CM and EM) CD4+	6.13E+04	9.34E+03
pooled CD45RA- (CM and EM) CD8+	7.63E+04	8.88E+03
PD-1+ CD8+ (6 healthy individuals)	7.78E+04	6.14E+03

CM, central memory; EM, effector memory.

Supplementary Table 3. CD2 mean expression in CD127±PD-1± TIL subsets from 19 CRC patients.

T cell subset	Molecules/cell	(+/-)SD
CD127$^+$PD-1$^-$ CD4$^+$	4.85E+04	1.27E+04
CD127$^+$PD-1$^+$ CD4$^+$	6.54E+04	1.50E+04
CD127$^-$PD-1$^+$ CD4$^+$	6.03E+04	1.59E+04
CD127$^-$PD-1$^-$ CD4$^+$	3.82E+04	7.10E+03
CD127$^+$PD-1$^-$ CD8$^+$	5.51E+04	1.17E+04
CD127$^+$PD-1$^+$ CD8$^+$	6.55E+04	1.86E+04
CD127$^-$PD-1$^+$ CD8$^+$	5.96E+04	2.11E+04
CD127$^-$PD-1$^-$ CD8$^+$	4.54E+04	1.04E+04

Supplementary Table 4. PD-1 mean expression in natural T-cell subsets in peripheral blood from 12 healthy individuals.

T cell subset	Molecules/cell	(+/-)SD
CM CD4+	4.84E+03	1.57E+03
EM CD4+	5.77E+03	1.52E+03
CM CD8+	5.48E+03	1.28E+03
EM CD8+	6.36E+03	1.26E+03
pooled CD45RA- (CM and EM) CD4+	5.30E+03	1.53E+03
pooled CD45RA- (CM and EM) CD8+	5.92E+03	1.23E+03

CM, central memory; EM, effector memory.

Supplementary Table 5. PD-1 mean expression in CD127⁻PD-1⁺ TIL subsets from 19 CRC patients.

T cell subset	Molecules/cell	(+/-)SD
CD127⁻PD-1⁺ CD4⁺	1.36E+04	6.34E+03
CD127⁻PD-1⁺ CD8⁺	1.45E+04	5.58E+03

Supplementary Table 6. CD58 mean expression in a human cell line and human primary myeloid cells from peripheral blood of two healthy individuals.

Cell type	CD58 molecules/cell	(+/-)SD
CF996 B cells line	8.98E+04	ND
Monocytes	5.30E+04	1.60E+03
Monocyted-derived DCs (immature)	6.33E+04	8.10E+03
Monocyted-derived DCs (mature)	1.15E+05	1.10E+04

ND, no data available

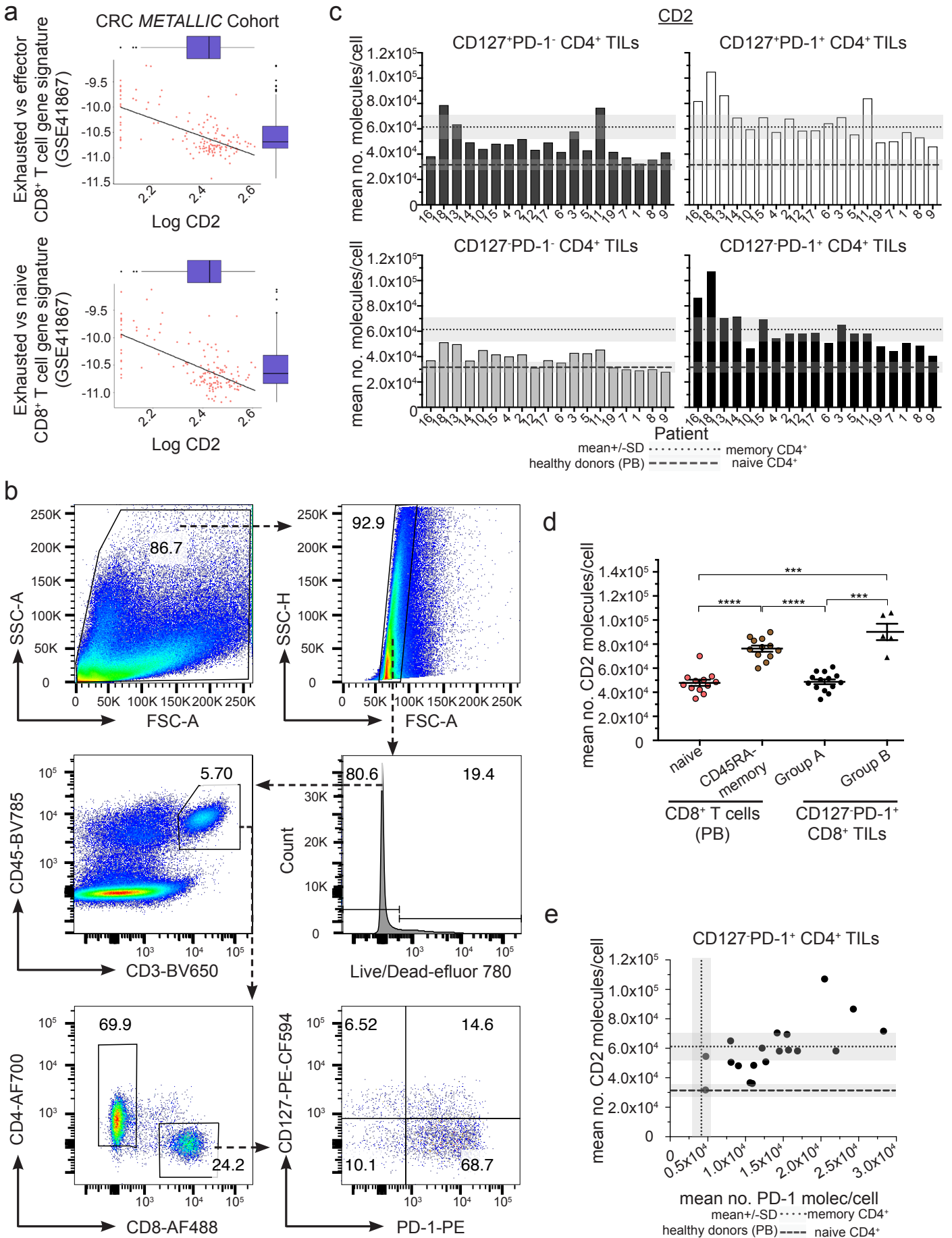# Fig. S1. CD8 exhaustion signature, CD2 gene expression and levels in CD4$^+$ and CD8$^+$ CRC TILs.

a CRC *METALLIC* Cohort

Exhausted vs effector CD8$^+$ T cell gene signature (GSE41867) vs Log CD2

Exhausted vs naive CD8$^+$ T cell gene signature (GSE41867) vs Log CD2

c CD2

CD127$^+$PD-1$^-$ CD4$^+$ TILs

CD127$^+$PD-1$^+$ CD4$^+$ TILs

CD127$^-$PD-1$^-$ CD4$^+$ TILs

CD127$^-$PD-1$^+$ CD4$^+$ TILs

mean no. molecules/cell

Patient

mean+/-SD ⋯⋯ memory CD4$^+$
healthy donors (PB) — — — naive CD4$^+$

b Flow cytometry gating

d mean no. CD2 molecules/cell

*** **** **** ***

naive | CD45RA$^-$ memory | Group A | Group B

CD8$^+$ T cells (PB) | CD127$^-$PD-1$^+$ CD8$^+$ TILs

e CD127$^-$PD-1$^+$ CD4$^+$ TILs

mean no. CD2 molecules/cell

mean no. PD-1 molec/cell

mean+/-SD ⋯⋯ memory CD4$^+$
healthy donors (PB) — — — naive CD4$^+$

Fig. S2. A unique ring pattern, "corolla", formed by CD2-CD58 interactions in the IS.
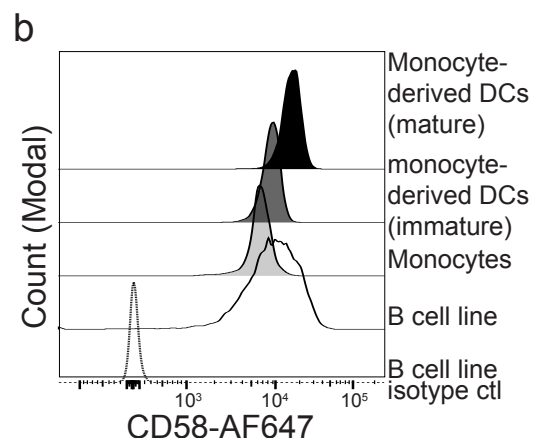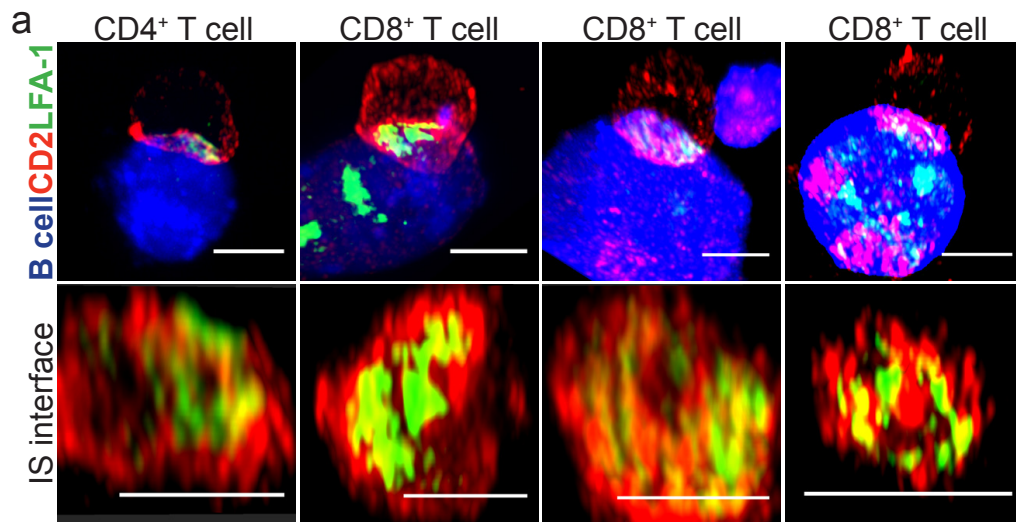
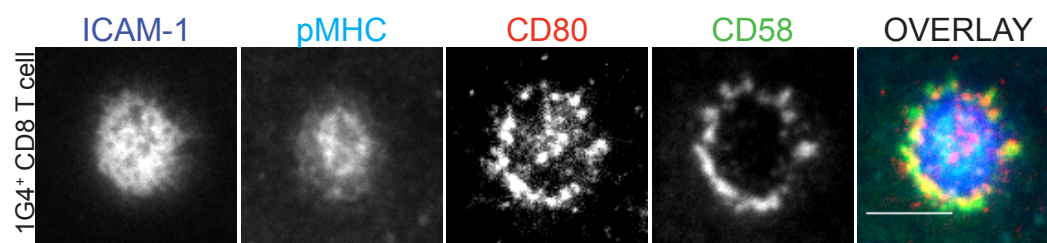## Fig. S3. pMHC-induced CD2 corolla captures ligated CD28

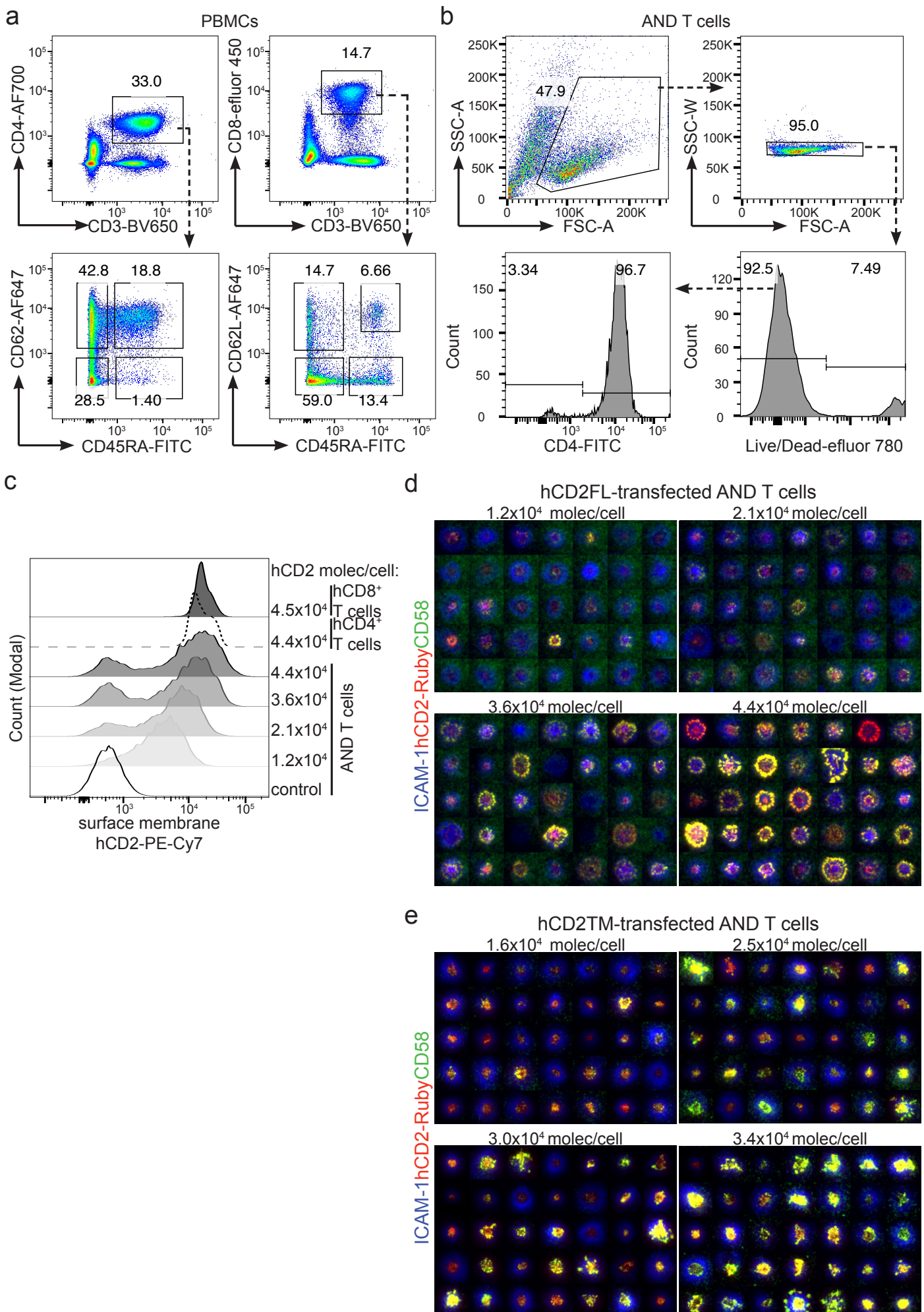# Fig. S4. CD2 expression levels determine corolla formation.

Fig. S5. CD127⁻PD-1⁺ CD8⁺ TILs from CRC patients are enriched in CD28⁻ TILs while CD127⁻PD-1⁺ CD4⁺ TILs are mainly CD28⁺.